

# An investigation of flow orientation on air–water two-phase flow in circular minichannel

Hemant B. Mehta · Jyotirmay Banerjee

Received: 10 March 2013 / Accepted: 18 March 2014 / Published online: 5 April 2014  
© Springer-Verlag Berlin Heidelberg 2014

**Abstract** Experimental investigations to establish the effect of flow orientations on gas–liquid two-phase flow patterns in minichannel is reported. Experimental test setup involves entry of air and water into the main channel through Y-junction inlet. Flow patterns are visualized for horizontal (0°), vertical (90°) upward, downward and angular ( $\pm 30^\circ$ ,  $\pm 45^\circ$ ,  $\pm 60^\circ$ ) orientations of the channel. The visualized images are utilized for establishing flow pattern maps for all the orientations. A comparative analysis of flow patterns for all the orientations reveal the influence of gravity in the surface tension dominating regimes of the flow.

## List of symbols

Bo	Bond number $Bo = \left( \frac{g(\rho_L - \rho_G)D_h^2}{\sigma} \right)$
Ca	Capillary number $Ca = \left( \frac{\mu(U_{SG} + U_{SL})}{\sigma} \right)$
Co	Confinement number $Co = \frac{1}{D_h} \sqrt{\frac{\sigma}{g(\rho_L - \rho_G)}}$
$D_h$	Channel hydraulic diameter
Eö	Eötvös number $Eö = \frac{g(\rho_L - \rho_G)D_h^2}{\sigma}$
$g$	Gravitational acceleration
$h_L$	Equilibrium liquid level
L	Laplace constant $L = \sqrt{\frac{\sigma}{g(\rho_L - \rho_G)}}$
LPM	Litre per minute
$Re_{SG/SL}$	Superficial Reynolds number $Re_{SG/SL} = \frac{\rho_{G/L} U_{SG/SL} D_h}{\mu}$

$U_{SG}$	Superficial gas velocity
$U_{SL}$	Superficial liquid velocity
YJ	Y-junction inlet
$\sigma$	Surface tension
$\rho_G$	Gas phase density
$\rho_L$	Liquid phase density
$\mu$	Dynamic viscosity

## 1 Introduction

Catalytic gas–liquid reaction is widespread among various chemical reactions. It occurs in chemical, biochemical, environmental, petrochemical and petroleum refining processes for extensive range of products. Different multi-phase reactors are used for gas–liquid reaction applications. Recently, significant research is being taken up to use monoliths as *multiphase reactors* in place of other reactors like trickle bed, slurry reactors etc. for mass transfer limited applications [1]. Monoliths comprise a block of thin, vertical, parallel channels of circular, rectangular, triangular, hexagon or more complex shapes and are separated by channel walls [2]. The preferred mode of operation for monolithic reactor is the intermittent flow of gas and liquid. Different researchers have identified this regime with different terminology such as “bubble-train flow” or “slug flow” by Thulasidas et al. [3, 4] and “Taylor flow regime” by Kreutzer et al. [5]. Slug flow regime provides excellent mass transfer at low pressure drop. Also augmented mass transfer is obtained with liquid superficial velocity of about 0.1 m/s as compared to 0.02 m/s or less for traditional multi-phase reactors. The higher liquid velocity reduces the diameter of the reactor vessels. Low pressure drop under high liquid throughput of a monolithic reactor prohibit the

H. B. Mehta · J. Banerjee (✉)  
Department of Mechanical Engineering, Sardar Vallabhbhai  
National Institute of Technology, Surat-7, Gujarat, India  
e-mail: jbaner@med.svnit.ac.in; jbaner@gmail.com

H. B. Mehta  
e-mail: hbm@med.svnit.ac.in

use of higher capacity pumps or compressors. Therefore, higher liquid velocity is achieved with more number of microsized channels of hydraulic diameter in the range of 0.3–3 mm [6].

Literature shows the dominance of surface tension force over gravitational force in such microscale channels. However, the definition of microscale channel is not yet clearly established. Significant research is carried out to establish a definition of microscale channel for which the surface tension effect will be dominant. Kew and Cornwell [7] proposed confinement number ( $Co$ ) for microchannel transition and suggested the threshold value of transition as  $Co = 0.5$ . Triplett et al. [8] proposed  $D_h \leq L$  as the transition criterion for microchannel flow where  $D_h$  is the channel hydraulic diameter and  $L$  is the Laplace constant. Besides confinement number ( $Co$ ), Eötvös number ( $Eö$ ) and Bond number ( $Bo$ ) are often used as microchannel transition criteria and correlated as  $Eö = Bo = 1/Co^2$ . Different values of the critical Eötvös number ( $Eö$ ) based on experimental conditions have been proposed in the literature. Bretherton [9] gave the value as  $Eö < 3.38$  ( $Co < 0.55$ ) and White and Beardmore [10] suggested the value around  $Eö_{cr} < 4$  ( $Co < 0.5$ ). For air–water system, the critical diameter is calculated as 2.7, 4.98 and 5.42 mm respectively. Mehendale et al. [11] has suggested 6 mm, Kandlikar and Grande [12] have suggested 3 mm while Chen et al. [13] found 2 mm as the threshold diameter for microscale channel. The above mentioned criteria fail to predict the threshold size of microscale channel which question the dominance of surface tension force in channel dimensions used in monolithic reactor.

The flow behavior of gas and liquid phase in each channel of monolithic reactor is observed to be identical. Moreover, the opaque nature of the monolith channel makes the visual observation impossible. These factors encourage the single channel investigations on gas–liquid two-phase flow. Other than *slug flow*, several other two-phase flow regimes are also observed in channels and they are *slug-annular flow*, *annular flow*, *churn flow* and *bubbly flow*. The hydrodynamics of these regimes observed in the channel essentially govern the design and performance of the monolith reactors. The development of these regimes are greatly influenced by the size and shape of the channel, physical properties and flow rates of the phases involved and more importantly orientations of the channel. Various prediction models for flow regime transition have been developed in horizontal, Taitel and Dukler [14], and in vertical, Taitel et al. [15], orientation of the pipe. The prediction models by Taitel and Dukler [15] however could not capture the different regimes in monolith channel. Based on their experiments, Barnea et al. [16] suggested that the prediction models of Taitel and Dukler [15] are

true for macroscale channels only. Two-phase flow behavior in horizontal minichannels of 1–5 mm diameter are studied by Fukano and Kariyaski [17], Coleman and Garimella [18], Triplett et al. [8], Damianides and Westwater [19], Yang and Shieh [20], Chen et al. [21], Hassan et al. [22], Lee and Lee [23], Venkatesan et al. [24]. They observed different flow patterns and proposed flow pattern maps. Gas–liquid two-phase flow with vertical orientations of the minichannel have been experimentally investigated by Mishima and Ishii [25], Galbiati and Andreini [26], Fukano and Kariyaski [17], Mishima and Hibiki [27], Zhao and Bi [28], Chen et al. [13], Hanafizadeh et al. [29]. The reported work on gas–liquid two-phase flow for downward microscale channel is rare to date. Biswas and Greenfield [30], Galbiati and Andreini [26], Thulasidas et al. [3, 4] and Tsoligkas et al. [1] experimentally investigated the downward flow behavior in different sized minichannels and developed the flow pattern maps. Based on the aforementioned literatures, the following questions are required to be answered:

1. Is surface tension a dominant force in channel dimensions used in monolithic reactors?
2. If surface tension is a dominant force, then what is its influence on flow patterns at different orientations of the channel?
3. How the orientation of the channel and established flow patterns augment the mass transfer processes in the reactor?

The aim of the present paper is to study the gas–liquid two-phase flow behavior in a monolithic minichannel and to identify standard flow patterns for various orientations of the minichannel. Isothermal investigations are carried out on air–water two-phase flow through 2.1 mm circular minichannel considering horizontal ( $\theta = 0^\circ$ ), vertical upward ( $\theta = +90^\circ$ ), vertical downward ( $\theta = -90^\circ$ ) and angular ( $\theta = \pm 30^\circ, \pm 45^\circ, \pm 60^\circ$ ) orientations of the minichannel. Based on the established flow patterns, flow pattern maps are developed for various orientations and compared with the appropriate transition maps and theoretical models available in literature. The effect of surface tension, recognized flow patterns and orientation of the channel on mass transfer mechanism in monolithic channel is also established.

## 2 Experimental setup

The experimental setup consists of a test section, air and water phase circuits and the image recording system. The test section is a straight circular glass tube of 2.1 mm internal diameter and is fixed on an acrylic sheet of 8 mm

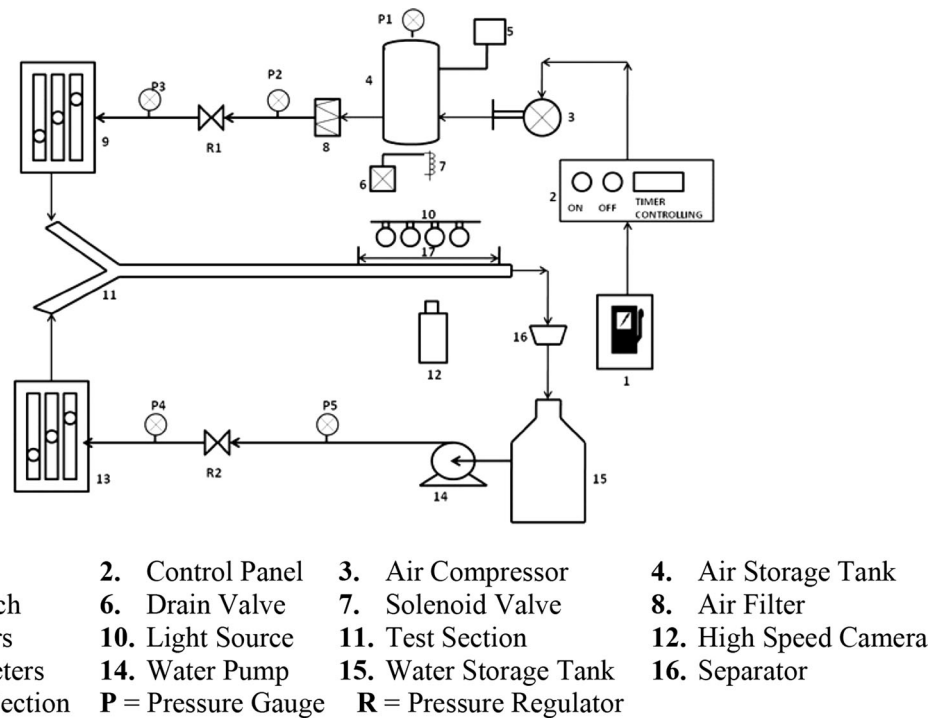


**Fig. 1** Schematic diagram of the experimental setup

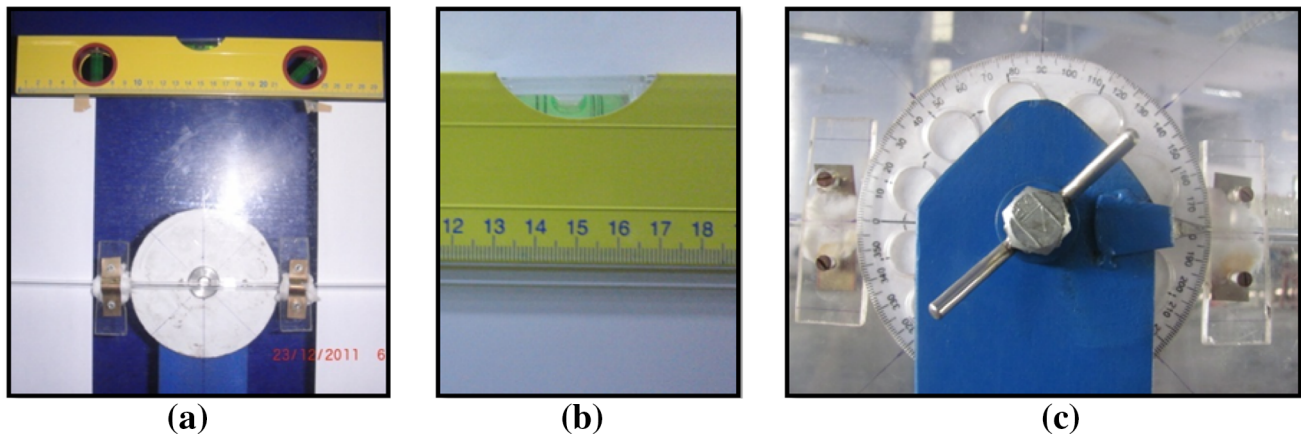


**Fig. 2** a, b Ensured horizontal position of the supporting acrylic sheet and test section using spirit level, c graduated angular scale

thickness pivoted centrally with collar bush. This allows the test section to be oriented through  $360^\circ$ . The schematic diagram of the experimental setup with a Y-junction test section is shown in Fig. 1. The perfect horizontal position of the test section and supporting acrylic sheet is ensured using spirit level as shown in Fig. 2a, b. This is followed by the alignment of the graduated angular scale to  $0^\circ$  as shown in Fig. 2c. Different orientations of the test section for which flow patterns are visualized are shown in Fig. 3.

The working fluids used are air and water. The density and dynamic viscosity at room temperature ( $25^\circ\text{C}$ ) are  $1.185\text{ kg/m}^3$  and  $1.848 \times 10^{-5}\text{ Pa s}$  for air while  $997.1$

$\text{kg/m}^3$  and  $8.936 \times 10^{-4}\text{ Pa s}$  for water respectively. The surface tension for water with air is found as  $0.072\text{ N/m}$ . Water is stored in a  $500\text{ l}$  capacity nonporous light weighted cylindrical polyethylene tank. Water is pumped using a  $0.5\text{ HP}$  pump. The water pressure is regulated with the help of a regulator and a bypass system to  $2\text{ kg/cm}^2$ . Three different rotameters with flow measuring ranges  $0.01\text{--}0.5\text{ LPM}$ ,  $0.2\text{--}2\text{ LPM}$  and  $0.4\text{--}5\text{ LPM}$  are connected to the inlet section for precise measurement of water flow rates. Water is then passed through a flexible PU pipe to the inlet of the test section. A non-return valve is placed at the exit of rotameters.

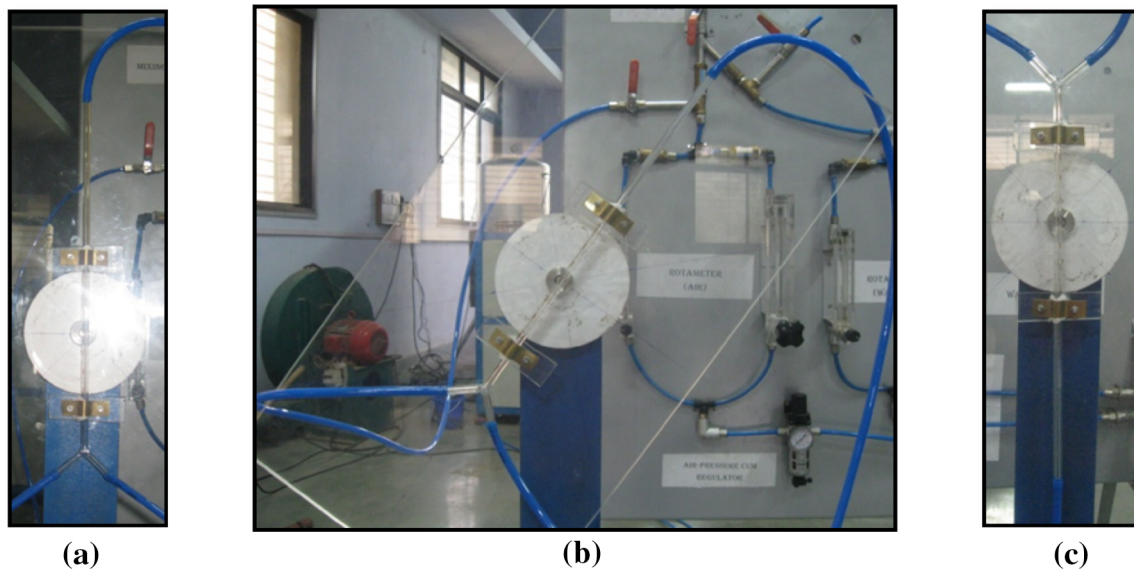


**Fig. 3** Different orientation of the test section **a** vertical upward, **b** angular, **c** vertical downward

Air is supplied to the test section using an air compressor. Air pressure is regulated to  $2 \text{ kg/cm}^2$  with a pressure regulator. It is subsequently passed through four different rotameters with flow measuring ranges of 0.04–0.5 LPM, 0–5 LPM, 1–20 LPM and 4–50 LPM. Air and water rotameters are calibrated using dry cal flow calibrator calibrated by Bios International Corporation, USA and ISA R.P. 16.6 standard. Accuracy of the rotameters at  $2 \text{ kg/cm}^2$  is within  $\pm 2 \%$  of its full scale reading. Air and water enter into the test section through Y-junction and are returned to the reservoir where they are separated and recycled. A variety of flow patterns are visualized by controlling the flow rates of air and water.

Flow patterns are visualized/captured at sufficient distance ( $L/D_h = 250$ ) from the inlet section to minimize the influence of entrance region. The flow patterns are observed with the help of image recording system consisting of two 1,000 Watts light source, high speed CMOS 9.1 megapixels camera, tripod stand, memory card and computer interface. The camera is set with the help of tripod stand which has the capability to adjust the camera height, angular rotation and up–down movement. The tripod has two spirit levels. One is kept for the stand while the other is to set the camera in perfect horizontal position. Captured two-phase flow images from memory card are transferred to personal computer for post processing.

### 3 Results and discussion

The experimental results for isothermal air–water two-phase flow in 2.1 mm Y-junction minichannel are discussed in this section. The first section is a discussion on

the flow patterns observed for horizontal ( $\theta = 0^\circ$ ), vertical ( $\theta = \pm 90^\circ$ ), and angular ( $\theta = \pm 30^\circ, \pm 45^\circ, \pm 60^\circ$ ) orientations of the minichannel. Here,  $\theta$  is the angle measured from the horizontal axis in upward (UW) and downward (DW) direction. This is followed by the development and comparison of flow pattern map for horizontal orientation. After ensuring the experimental procedure based on the validation with literature for horizontal orientation, flow patterns are established and flow pattern maps are developed for all upward (UW) and downward (DW) orientations.

#### 3.1 Flow regimes

The observed flow patterns for various orientations of the minichannel are presented in Fig. 4. Different flow patterns are observed for superficial velocities in the range of 0.0459–1.3772 m/s for water and 0.1836–13.7722 m/s for air. The superficial Reynolds number ( $Re_{SG/SL}$ ) range for water is 118–3,245 while for air is 24–1,852. The capillary number ( $Ca$ ) is in the range of 0.003–0.19 and Bond number is found as 0.60. The uncertainty of 5.24 % is found for flow velocities and 3.22 % for Reynolds number. Total seven flow patterns such as slug, slug-bubbly, bubbly, slug-annular, annular, churn and wavy stratified are observed. The observation is carried out by keeping air flow rate constant and changing the water flow rate. The images shown in Fig. 4a–c are captured using high speed camera at 210 frames per second (fps) and  $480 \times 360$  recorded pixels while in Fig. 4d are captured at 1,000 fps and  $224 \times 64$  recorded pixels. Air–water mixture makes entry from the left and travel to right in all the images shown here.

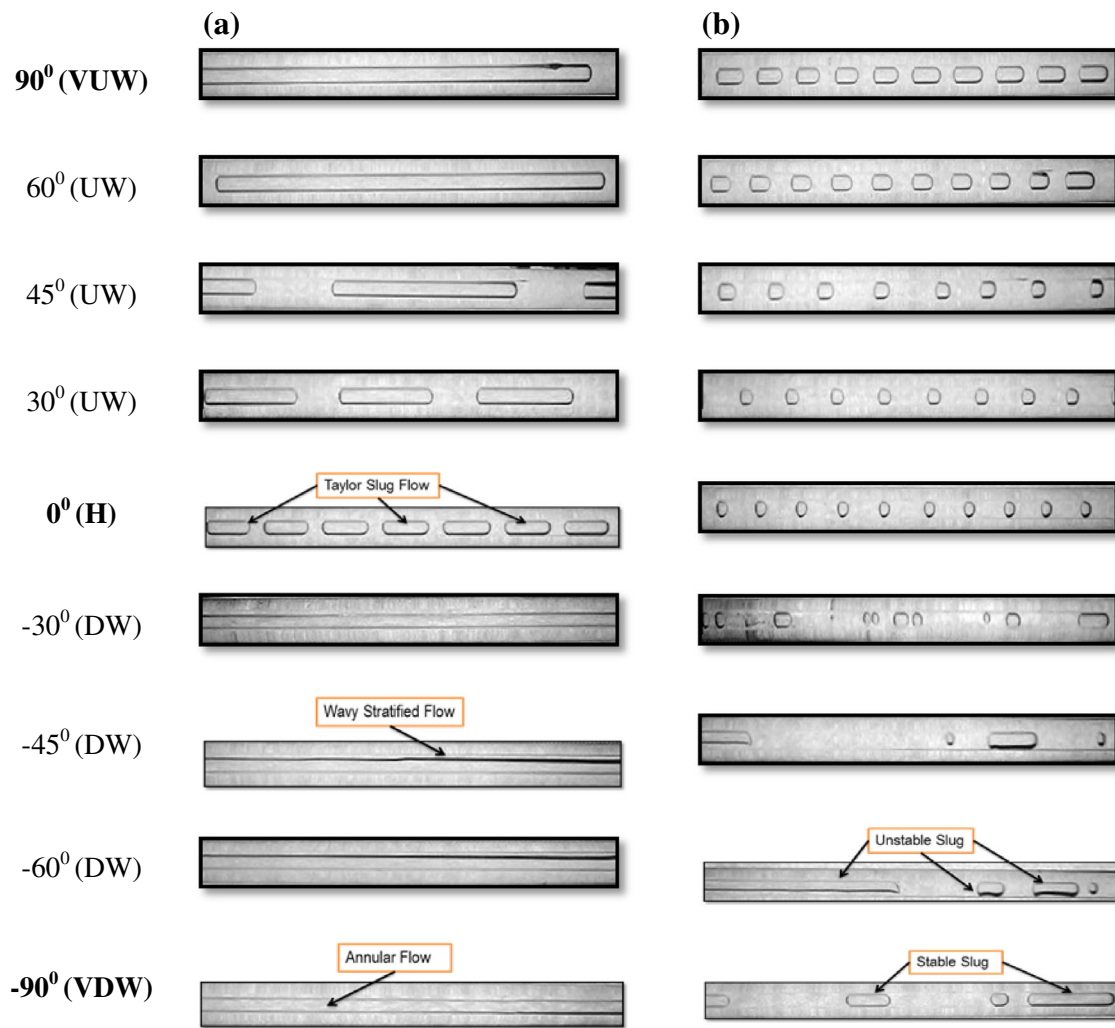


**Fig. 4** Observed flow patterns for various orientations of the minichannel. **a**  $U_{SG} = 0.3673$  m/s  $U_{SL} = 0.0459$  m/s, **b**  $U_{SG} = 0.1836$  m/s  $U_{SL} = 0.2295$  m/s, **c**  $U_{SG} = 1.8363$  m/s  $U_{SL} = 0.0459$  m/s, **d**  $U_{SG} = 13.7722$  m/s  $U_{SL} = 1.3772$  m/s

Taylor slug (capillary slug) is observed at low liquid and gas flow rate for horizontal (H) position of the minichannel as shown in Fig. 4a. The images shown in Fig. 4a are captured at 210 fps and  $480 \times 360$  recorded pixels. With increase in upward (UW) and vertical upward (VUW) orientations, the length ratio of gas bubble to unit cell (gas bubble and liquid slug) is found to increase. It is due to gravity force becoming dominant over surface tension force for upward (UW) orientation. This delays the break-up of gas bubbles at the Y-junction of the minichannel. It is found that stratified flow is difficult to observe in small diameter minichannel. However, wavy stratified flow is observed for downward (DW) orientations. Annular flow is observed for vertical downward (VDW) orientation of the channel.

As shown in Fig. 4b, Taylor slug changes to bubbly flow for horizontal (H) position when gas flow rate is

reduced to half and water flow rate is increased to five times the flow conditions mentioned in Fig. 4a. Increase in liquid flow rate increases the liquid drag force and accelerates the gas bubble detachment process at the channel inlet. Bubbles do not collide or coalesce with each other and move with same speed as that of the liquid. This shows the homogeneous condition of two-phase flow. Bubbly flow changes to stable slug flow for UW and VUW orientations and slug length is found to increase with upward orientation. This demonstrates the dominance of gravity force over surface tension force. Slug-bubbly flow is observed for DW and VDW orientations. Unstable slug is observed in slug-bubbly flow for DW orientations which is later converted to stable slug for VDW orientation. Different flow regimes observed at the same flow conditions represent the effect of flow orientation on two-phase flow in minichannel. This in turn

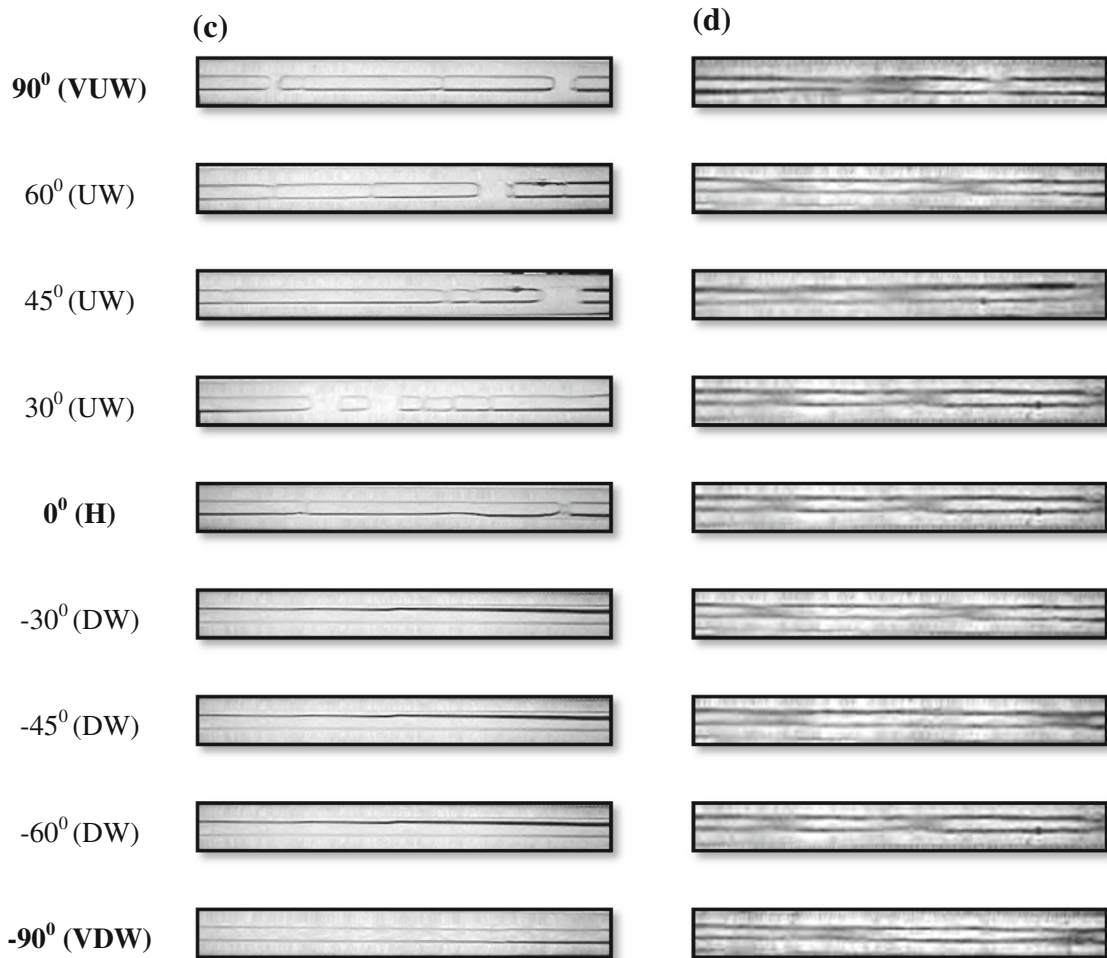


**Fig. 4** continued

shows the dominance of gravitational force over surface tension force for surface tension dominating region.

As shown in Fig. 4c, slug flow changes to slug-annular flow for horizontal (H) position and remains same for all upward orientations. These flow regimes are observed when gas flow rate is increased by five times keeping water flow rate constant compared to flow conditions mentioned in Fig. 4a. Wavy stratified flow is observed for all downward (DW) orientations while annular flow is observed for vertical downward (VDW) orientation. As per Fig. 4a, c, wavy stratified flow is the recognized flow pattern in all DW orientations while annular flow is the established flow pattern in VDW orientation at low liquid flow rate. At low gas flow rate, the liquid flow is like the falling film and converts into typical annular flow at high gas flow rate when liquid flow rate is kept low. Churn flow is observed at very high gas and liquid flow rates irrespective of flow orientations and shown in Fig. 4d. It signifies that flow orientation has no remarkable effect on this flow regime.

## 3.2 Flow regime maps

### 3.2.1 Horizontal (H) orientation

The flow pattern map developed for horizontal position of the minichannel is shown in Fig. 5a. At low gas and liquid velocities, slug flow is observed. Slug flow changes to annular flow with the increase in gas velocity. Bubbly flow and churn flow are observed at high liquid superficial velocity. Slug flow to annular flow transition is mushy due to the dominance of these regimes over each other alternatively within certain range of gas velocity in the test section and hence this region is termed as slug-annular regime. Here, inertia force try to become dominant but surface tension or interfacial forces are still strong in this regime. At higher gas flow velocities, inertia forces predominate over interfacial forces and hence annular flow is observed.

The developed flow pattern maps are compared with the theoretical flow pattern map proposed by Taitel and Dukler

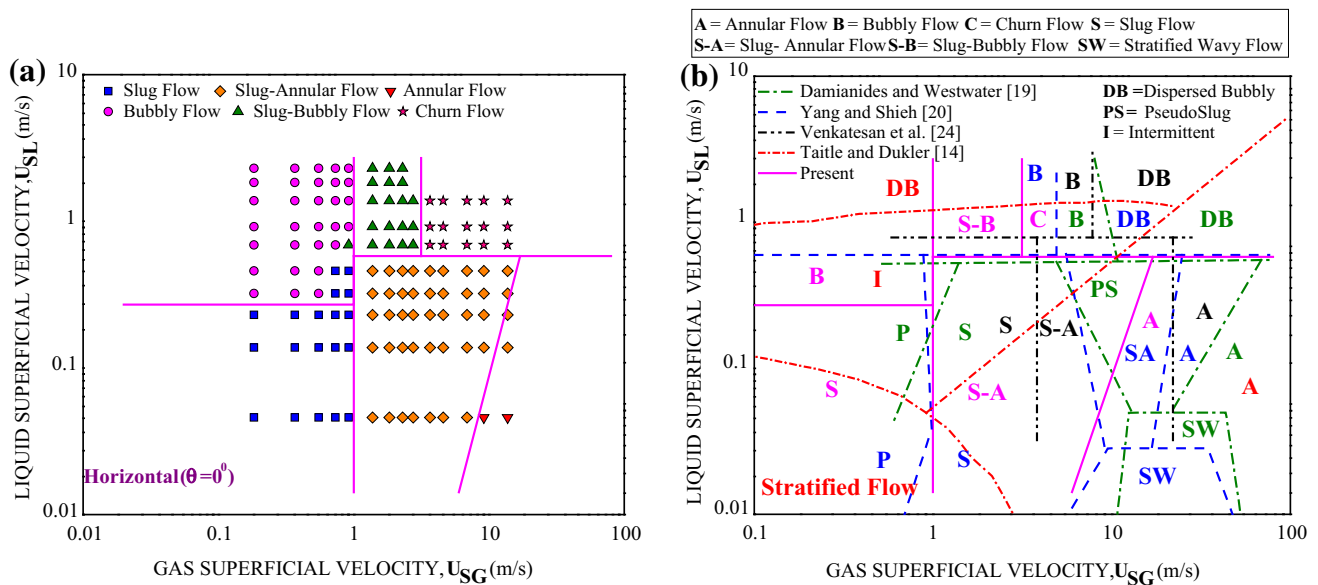


**Fig. 5** Flow pattern map for horizontal orientation of the minichannel. **a**  $\theta = 0^\circ$ , **b** comparison with available literature

[14] as well as experimental flow pattern maps of Damianides and Westwater [19], Yang and Shieh [20] and Venkatesan et al. [24]. Taitel and Dukler [14] presented the theoretical transition criteria for conventional pipe of 25.4 mm internal diameter as shown in Fig. 5b. Yang and Shieh [20] used 2 mm mini tube with a mixer of a cylindrical chamber of 12.7 mm internal diameter and 50.8 mm length. The agitated mixture of air and water was supplied through a stainless steel mesh filter of 40,000 pores/in<sup>2</sup>. Venkatesan et al. [24] used 1.7 mm glass tube with a T-junction inlet in which air mixed with water through four holes of 1 mm diameter. The present results are obtained with direct mixing of air–water through Y-junction inlet which gives smaller mixing volume and reasonably good mixing quality of air–water. This was done following the numerical investigations by Qian and Lawal [31] and experimental study by Shao et al. [32]. Slug to bubbly flow transition is observed little early for lower range of gas flow rates. As the gas flow rate is increased, the transition line agrees well with the data of Damianides and Westwater [19] and Yang and Shieh [20]. Wavy-stratified regime shown by Damianides and Westwater [19] and Yang and Shieh [20] is not observed in the present experiment for horizontal position of the minichannel. This is in line with the observations reported by Venkatesan et al. [24]. Plug and slug regime cover wide range of gas and liquid velocities in the flow pattern maps of Damianides and Westwater [19] and Yang and Shieh [20]. In fact, plug flow defined by Damianides and Westwater [19] and Yang and Shieh [20] and slug flow observed in the present experiment are similar. Early transition of observed flow regimes in the present map ( $D_h = 2.1$  mm) compared to the observations reported by Venkatesan et al. [24]

obtained on 1.7 mm mini tube is due to the difference in diameter. The developed flow pattern map in this work is found in good agreement with the literature cited in Fig. 5. Taitel and Dukler [14] reported that in horizontal conventional channel, the liquid wets and climb the tube wall as shown in Fig. 5b. However in microscale channel the climbing liquid creates a complete liquid bridge in the presence of capillary force which initiates the intermittent flow. The intermittent-dispersed transition boundary is observed to shift to higher value of water velocity. They also suggested that liquid level in the stratified equilibrium flow will only decide the development of intermittent or annular flow. According to their prediction, intermittent flow will develop when the equilibrium liquid level ( $h_L$ ) in the tube of internal diameter ( $D_h$ ) is above the tube centreline. Annular or annular-dispersed flow will develop when the ratio is  $h_L/D_h < 0.5$ . The present observations on the contrary depicts that the development of transition boundary from intermittent to annular regime depends mostly on air velocity unlike water velocity as was predicted by the model of Taitel and Dukler.

### 3.2.2 Upward (UW) and vertical upward (VUW) orientation

The flow pattern maps developed for different UW orientations are shown in Fig. 6. The flow pattern maps developed for 30° and 45° orientations are found alike. The flow pattern map developed for 60° orientation is shown in Fig. 6b. Here, slug to bubbly transition is observed to shift little upward to higher liquid velocity for 60° compared to 30° and 45° orientations of the channel. This transition is more shifted to upward for VUW (90°) orientations and

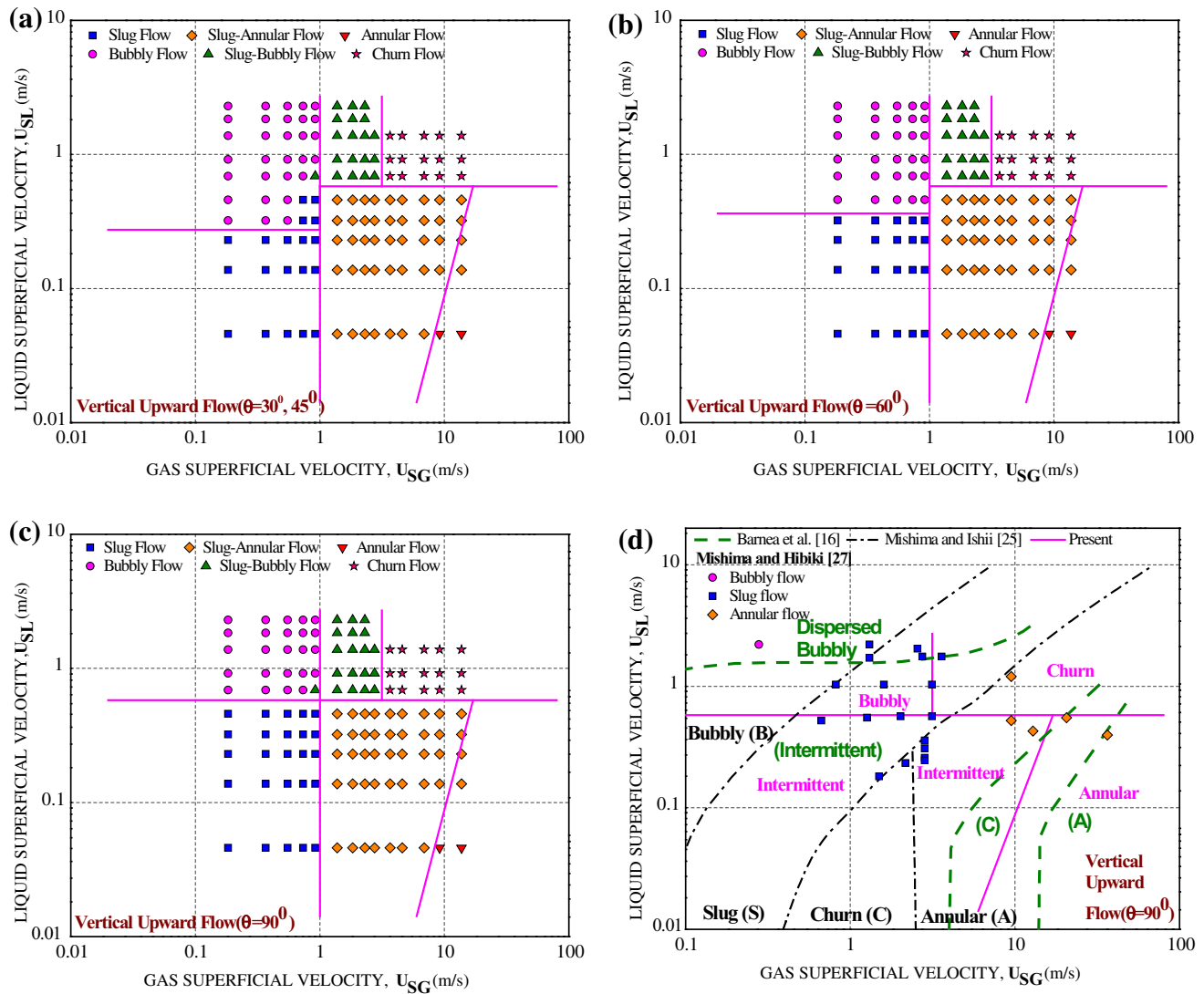


**Fig. 6** Flow pattern map for upward orientations of the minichannel. **a**  $\theta = 30^\circ, 45^\circ$ , **b**  $\theta = 60^\circ$ , **c**  $\theta = 90^\circ$ , **d** comparison of  $\theta = 90^\circ$  flow with the available literature

shown in Fig. 6c. All other flow regime transition lines are found to remain unaltered for UW and VUW orientations of the minichannel. The present transition boundaries for VUW orientation, Fig. 6d, are compared with the results of Barnea et al. [16] obtained for 4 mm circular pipe, Mishima and Hibiki [27] obtained for 2.05 mm mini tube and the transition model proposed by Mishima and Ishii [25] for conventional tube. Intermittent flow shown by Barnea et al. [16] combines the elongated bubble and slug flow. The present experiment on the other hand combines the slug and slug-annular flow for 2.1 mm diameter round tube. Barnea et al. [16] compared the results with the theoretical model of Taitel et al. [15] and found to be in good agreement. Moreover, they did not find remarkable effect of pipe diameter in VUW orientation. All the present transition lines in Fig. 6d qualitatively agree with the

experimental and theoretical work of Barnea et al. [16] and prediction model of Mishima and Ishii [25] based on the subjectivity of flow regime identification. The experimental results of Mishima and Hibiki [27] are also found to be consistent with the developed flow pattern map for VUW orientation. The authors believe that in the absence of flow pattern maps for UW orientations, i.e.,  $30^\circ, 45^\circ$  and  $60^\circ$ , these developed flow pattern maps could be a guide line for adiabatic two-phase flow investigations in inclined micro-scale channel and will reasonably predict the flow regimes.

### 3.2.3 Downward (DW) and vertical downward (VDW) orientation

The flow pattern maps developed for DW and VDW orientations of the minichannel are shown in Fig. 7. In



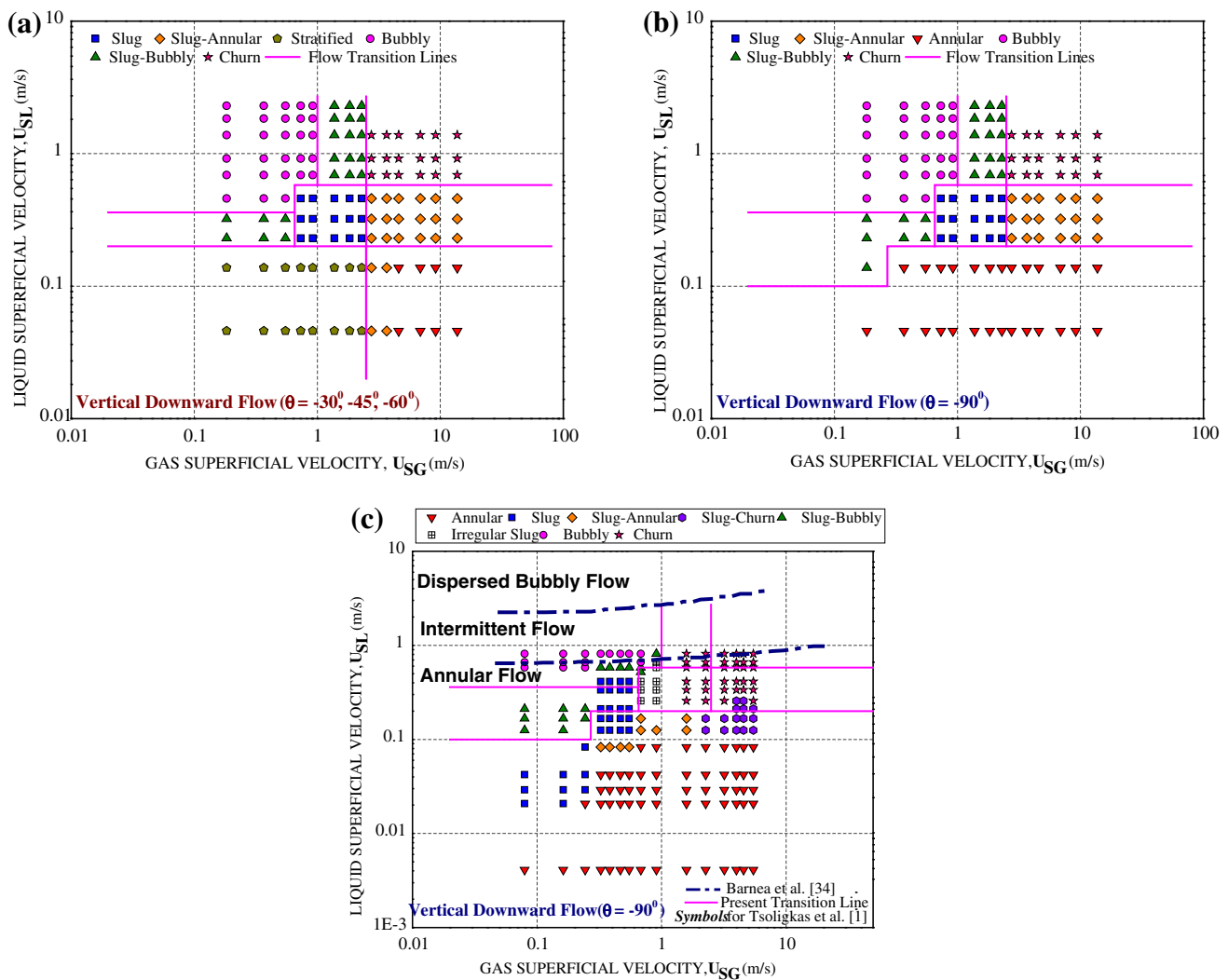


**Fig. 7** Flow pattern map for downward orientations of the minichannel. **a**  $\theta = -30^\circ, -45^\circ, -60^\circ$ , **b**  $\theta = -90^\circ$ , **c** comparison of  $\theta = -90^\circ$  flow with the available literature

order to minimize the downstream instabilities, tube inlet design where liquid and gas premix is very important. Biswas and Greenfield [30] used Y-junction whereas Galbiati and Andreini [26] used conical section of glass for water and glass needle for air which could move axially in tapered section connected directly to the calming section. Triplett et al. [8] used a mixer of cross-shaped wherein gas phase entry was radial through two holes of 1.59 mm diameter. Serizawa et al. [33] used the co-flow mixer in which gas entered through an annulus while liquid entered through the centre core (pipe). A mixer of various T-junctions was used by Thulasidas et al. [3, 4] while gas nozzle type of mixer was used by Bi and Zhao [28]. In the present experiments, Y-junction channel is used which provides better premixing quality of air–water and minimizes the downstream instabilities.

At lower liquid flow rate, wavy stratified flow is observed for DW orientations of the channel for certain range of gas flow rate while annular flow is observed for VDW throughout the range of gas flow rate. At these flow conditions, wavy stratified and annular flow is converted first to unstable slug flow which finally turns into bubbly flow with increase in liquid flow rate. At higher gas and liquid flow rates, churn flow is observed. The existence of stratified flow in DW orientation confirms the reported results of Biswas and Greenfield [30]. In VDW channel, a symmetric falling film of liquid is observed when liquid is allowed to flow at lower flow rate in the absence of gas flow rate. This falling film converts into annular flow with gas flow rate. Hence, annular flow becomes the usual flow regime in VDW channel at lower liquid flow rate and transition of flow regimes starts from annular flow regime. With increase in liquid flow rate, liquid hold up increases

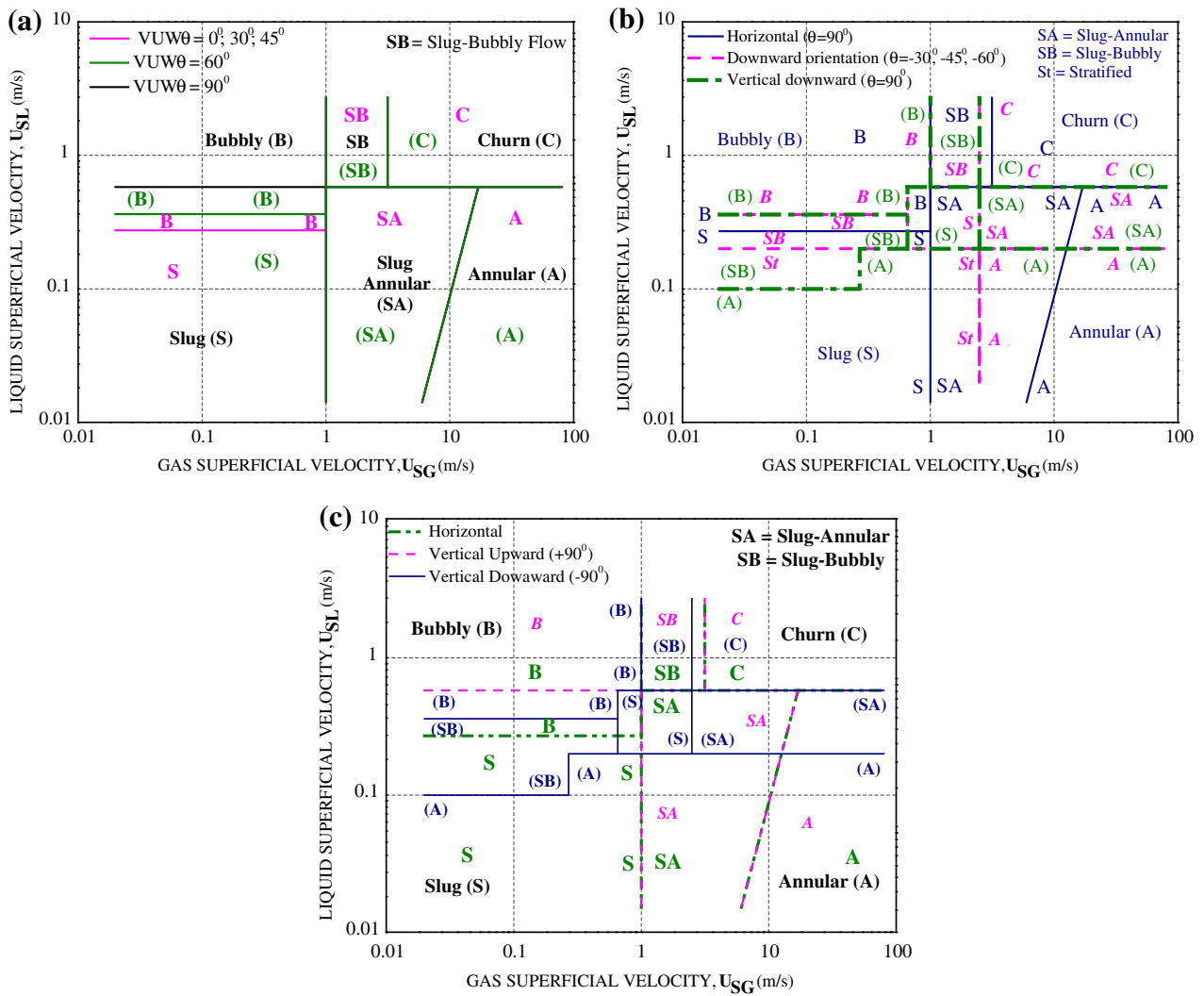


**Fig. 8** Comparison of flow pattern map for various orientations of the minichannel. **a** Horizontal and upward, **b** horizontal and downward, **c** horizontal, vertical upward and vertical downward

and slug formation starts. Further increase in liquid hold up breaks the gas slug and bubbly flow is observed. The developed flow regime transition boundaries for VDW orientation and its comparison with the cited literature are shown in Fig. 7c. Here, solid lines stand for present transition criteria, dashed lines show the lines of transition reported by Barnea et al. [34] observed for 25.5 mm conventional pipe and symbols represent the experimental data of Tsoiligkas et al. [1] for 2 mm hydraulic diameter of rectangular channel. According to Barnea et al. [34], the transition of annular flow to slug flow is observed when liquid void fraction in downward annular flow is twice the slug holdup. This transition criteria is not valid for small channels and found over predicted. Conversely, the experimental data of Tsoiligkas et al. [1] for small channel is in good agreement with the present results. This confirms that the criteria proposed by Barnea et al. [34] over predict

the transition boundaries. This signifies the macro to micro-sized scaling down effect of channels.

### 3.2.4 Comparison for different orientations

Comparison of flow pattern maps for various flow orientations of the minichannel is shown in Fig. 8. It is observed from Fig. 8a that transition from slug to bubbly is gradual and achieved at increased liquid flow rate with increase in angular (UW) orientations. All other transition boundaries are found unchanged for UW and VUW orientations compared to horizontal flow pattern transition map.

As shown in Fig. 8b, slug flow is found the recognized flow pattern for horizontal (H) channel at low gas and liquid flow rates. Slug flow changes to wavy stratified flow for all DW orientations and finally converts to falling film

annular flow for VDW orientation. With increase in liquid flow rate at low gas flow rate, these patterns change to bubbly flow for H, DW and VDW orientations of the channel. Increase in gas flow rate at low liquid flow rate, slug flow changes to slug-annular flow in horizontal (H) channel. At these conditions, wavy stratified flow changes to annular flow for DW orientations while falling film annular flow, observed for VDW orientation, is changed to typical annular flow at higher gas flow rate. At very high gas and liquid flow rate, churn flow is observed for all the flow orientations of the minichannel. The comparison of flow patterns for horizontal, VUW and VDW orientations is shown in Fig. 8c. The results demonstrate that flow orientation has little effect from horizontal to VUW orientations. However, for VDW orientation gravity dominated flow i.e. DW flow significantly affects the flow pattern map compared to H and VUW orientation.

#### 4 Conclusion

The present study is an experimental investigation to observe two-phase flow patterns in the channel of monolithic reactor for nine different orientations. The flow behaviour is investigated with air–water two-phase flow in a minichannel of 2.1 mm internal diameter. Seven different flow regimes are identified and flow pattern maps are developed for horizontal, upward and downward orientations of the minichannel. The conclusions are drawn as follows:

1. Slug flow is established as the flow pattern at lower gas and liquid flow rates for horizontal (H) and all upward (UW and VUW) orientations of the minichannel. The length ratio of gas bubble to unit cell (gas bubble and liquid slug) is found to increase with upward orientation. Slug regime on flow pattern map is expanded with increase in liquid velocity from H to all UW orientation. This provides short diffusion path which enhances the gas–solid mass transfer right from H to all UW orientation of the channel.
2. The liquid slug length is found smaller compared to gas bubble length with H and all UP orientations. Short slug length creates higher interfacial area improves the mixing in liquid slug and increases the gas–liquid mass transfer for H to all UW orientation of the channel.
3. Maximum mass transfer can be obtained with vertical upward orientation of the monolith reactor compared to H and all UW orientation when operated with slug flow regime.
4. The transition of other flow regimes is found unchanged with UW orientation. This provides constant mass transfer with increased pressure drop when the reactor is operated with flow regimes other than slug flow regime.
5. Wavy stratified flow is observed at lower gas and liquid flow rates for downward (DW) orientations of the minichannel. Increase in gas flow rate forms typical annular flow pattern for DW and VDW orientations. The presence of stratified flow in DW orientation limits the use of monolith reactor in DW orientation due to its adverse effect on the mass transfer mechanism.
6. Film type annular flow is observed at lower gas and liquid flow rate for vertical downward (VDW) orientation which converts into typical annular flow pattern with increased gas flow rate. The transition boundaries remain unaltered for all downward orientation of the channel which shows very little effect of orientation on DW flow pattern map. The liquid film near wall will increase the interfacial area and shorten the diffusion path. This will increase the gas–solid mass transfer when monolith reactor is operated in VDW orientation with annular flow regime and offer low pressure drop.
7. In the absence of flow pattern maps for inclined channels, the developed flow pattern maps for UW and DW orientations could become the guide lines for further investigation on two-phase flow through micro-scale channels.

**Acknowledgments** The authors would like to acknowledge the authorities of the Sardar Vallabhbhai National Institute of Technology, Surat for providing financial support for the development of Advanced Fluid Dynamics Lab where this minichannel based experiments are conducted.

#### References

1. Tsoligkas AN, Simmons MJH, Wood J (2007) Influence of orientation upon the hydrodynamics of gas–liquid for square channels in monolith supports. *Chem Eng Sci* 62:4365–4378
2. Roy S, Bauer T, Al-Dahhan M, Lehner P, Turek T (2004) Monoliths as multiphase reactors: a review. *AIChE J* 50(11):2918–2938
3. Thulasidas TC, Abraham MA, Cerro RL (1997) Flow patterns in liquid slugs during bubble–train flow inside capillaries. *Chem Eng Sci* 52:2947–2962
4. Thulasidas TC, Abraham MA, Cerro RL (1999) Dispersion during bubble–train flow in capillaries. *Chem Eng Sci* 54:61–76
5. Kreutzer MT, Kapteijn F, Moulijn JA, Heizwolf JJ (2005) Multiphase monolith reactors: chemical reaction engineering of segmented flow in microchannels. *Chem Eng Sci* 60:5895–5916
6. Abiev RSh, Lavretsov IV (2012) Intensification of mass transfer from liquid to capillary wall by Taylor vortices in minichannels, bubble velocity and pressure drop. *Chem Eng Sci* 74:59–68
7. Kew P, Cornwell K (1997) Correlations for prediction of flow boiling heat transfer in small-diameter channels. *Appl Therm Eng* 17:705–715
8. Triplett KA, Ghiaasiaan SM, Abdel-Khalik SI, Sadowski DL (1999) Gas–liquid two-phase flow in microchannels part I: two-phase flow patterns. *Int J Multiph Flow* 25:377–394

9. Bretherton FP (1961) The motion of long bubbles in tubes. *J Fluid Mech* 10:167–188
10. White E, Beardmore R (1962) The velocity of rise of single cylindrical air bubbles through liquids contained in vertical tubes. *Chem Eng Sci* 17:351–361
11. Mehendale SS, Jacobi AM, Ahah RK (2000) Fluid flow and heat transfer at micro- and meso-scales with application to heat exchanger design. *Appl Mech Rev* 53:175–193
12. Kandlikar SG, Grande WJ (2003) Evolution of microchannel flow passages: thermo hydraulic performance and fabrication technology. *Heat Transf Eng* 24(1):3–17
13. Chen L, Tian YS, Karayiannis TG (2006) The effect of tube diameter on vertical two-phase regimes in small tubes. *Int J Heat Mass Transf* 49:4220–4230
14. Taitel Y, Dukler AE (1976) A model for predicting flow regime transitions in horizontal and near horizontal gas liquid flow. *AIChE J* 22(1):47–55
15. Taitel Y, Barnea D, Dukler AE (1980) Modelling flow pattern transitions for steady upward gas–liquid flow in vertical tubes. *AIChE J* 26:345–354
16. Barnea D, Luninski Y, Taitel Y (1983) Flow pattern in horizontal and vertical two phase flow in small diameters pipes. *Can J Chem Eng* 61(5):617–620
17. Fukano T, Kariyasaki A (1993) Characteristics of gas–liquid two-phase flow in a capillary. *Nucl Eng Des* 141:59–68
18. Coleman JW, Garimella S (1999) Characterization of two-phase flow patterns in small diameter round and rectangular tubes. *Int J Heat Mass Transf* 42:2869–2881
19. Damianides C, Westwater JW (1988) Two phase flow patterns in a compact heat exchanger and in small tubes. In: Proceedings of second U. K. national conference on heat transfer, vol II, glasgow, September 14–16, 1988, Mechanical Engineering Publications, London, pp 1257–1268
20. Yang CY, Shieh CC (2001) Flow pattern of air–water and two-phase R-134a in small circular tubes. *Int J Multiph Flow* 27:1163–1177
21. Chen WL, Twu MC, Pan C (2002) Gas–liquid two-phase flow in micro-channels. *Int J Multiph Flow* 28:1235–1247
22. Hassan I, Vaillancourt M, Pehlivan K (2005) Two-phase flow regime transitions in microchannels: a comparative experimental study. *Microscale Therm Eng* 9:165–182
23. Lee CY, Lee SY (2008) Influence of surface wettability on transition of two-phase flow pattern in round mini-channels. *Int J Multiph Flow* 34:706–711
24. Venkatesan M, Das SK, Balakrishnan AR (2011) Effect of diameter on two-phase pressure drop in narrow tubes. *Exp Thermal Fluid Sci* 35:531–541
25. Mishima K, Ishii M (1984) Flow regime transition criteria for upward two-phase flow in vertical tubes. *Int J Heat Mass Transf* 27(5):723–737
26. Galbiati L, Andreini P (1992) Flow pattern transition for vertical downward two phase flow in capillary tubes. Inlet mixing effects. *Int Commun Heat Mass Transf* 19:791–799
27. Mishima K, Hibiki T (1996) Some characteristics of air–water two-phase flow in small diameter vertical tubes. *Int J Multiph Flow* 22:703–712
28. Zhao TS, Bi QC (2001) Co-current air–water two-phase flow patterns in vertical triangular microchannels. *Int J Multiph Flow* 27:765–782
29. Hanafizadeh P, Saidi MH, Gheimasi AN, Ghanbarzadeh S (2011) Experimental investigation of air–water two-phase flow regimes in vertical mini pipe. *Sci Iran B* 18(4):923–929
30. Biswas J, Greenfield PF (1985) Two-phase flow through vertical capillaries-existence of a stratified flow pattern. *Int J Multiph Flow* 11(4):553–563
31. Qian D, Lawal A (2006) Numerical study on gas and liquid slugs for Taylor flow in a T-junction microchannel. *Chem Eng Sci* 61:7609–7625
32. Shao N, Gavriilidis A, Angeli P (2011) Effect of inlet conditions on Taylor bubble length in microchannels. *Heat Transf Eng* 32(13–14):1117–1125
33. Serizawa A, Feng Z, Kawara Z (2002) Two-phase flow in microchannels. *Exp Thermal Fluid Sci* 26:703–714
34. Barnea D, Shoham O, Taitel Y (1982) Flow pattern transition for vertical downward two phase flow. *Chem Eng Sci* 37(5):741–744